Giant Low Surface Brightness Galaxies as Merger Remnants

Peter Yoachim[1], Denise Shmitz[1], Sarah Loebman[2], SungWon Kwak[1], Victor P. Debattista[3]

ABSTRACT

We present IFU observations of the giant low surface brightness galaxies Malin 2 and UGC 6614. We fit the stellar dynamics of these systems and compare their spatially resolved spectra to star formation history models. We argue that Malin 2 and UGC 6614 are normal elliptical galaxies which have undergone a high angular momentum merger which formed their GLSB disks, making them unique systems for probing the dark matter halos of elliptical systems. We find the stellar dynamics are consistent with earlier measurements of the GLSB H I disks. The stellar populations of the GLSB disks are dominated by old metal-poor stars, while the central ellipticals are metal rich.

Subject headings: galaxies: kinematics and dynamics — galaxies: formation — galaxies: structure

1. Introduction

Since the discovery of Malin 1 (Bothun et al. 1987), giant low surface brightness galaxies (GLSB) have presented a unique problem for galaxy formation theories. Low surface brightness (LSB) galaxies are typically defined as disks with central surface brightnesses fainter than 23 B mag arcsec^2. These disks are incredibly large, with Malin 1 being detected to a radius of over 100 kpc (Moore & Parker 2006). It is difficult to imagine how a stellar disk could form within a merger-driven ΛCDM cosmology.

A wide variety of formation scenarios have been proposed for GLSB systems. Mapelli et al. (2008) form GLSB-like galaxies via the fading of collisional ring galaxies xxx-expand this a bit.

Meanwhile, observers tend to classify GLSB systems as normal spirals. Das (2013) concludes that GLSB systems are an extreme form of late type spiral galaxies. Similarly,

[1]Department of Astronomy, University of Washington, Box 351580, Seattle WA, 98195

[2]XXX-U Mich

[3]Jeremiah Horrocks Institute, University of Central Lancashire, Preston PR1 2HE, UK. RCUK Fellow

Kasparova et al. (2014) claim that the large dark matter scale of Malin 2 can explain it's features.

XXX-add discussion of possibility the centers of GLSBs are normal galaxies.

In this paper, we use IFU spectroscopy to measure the star formation histories of two GLSB systems.

The problem with considering GLSB systems as normal spirals is that they are clearly outliers when one considers the specific angular momentum of the systems. The difference between high surface brightness (HSB) spirals and low surface brightness spirals (LSB), could simply be an issue of specific angular momentum. xxx-this goes in the discussion I think. Dutton & van den Bosch (2012) is a nice paper on how disk galaxies get their angular momentum–I'll need to make a calc of how much J is in the GLSB disks to compare it.

GLSBs are typically classified as spriral galaxies (Das 2013), however, high resolution imaging of Malin 1 has shown that the central region appears to be a normal

Raskutti et al. (2014) use VIRUS-P to look at stellar halo kinematics of massive ellipticals. Lots of good stuff on fast/slow rotators. Also a very nice plot showing the radial gradients in age and metallicity as measured from Lick indices. They don't see any sharp transition like I do, all very smooth age and metal curves.

Kasparova et al. (2014) has an amazing analysis of Malin 2. They combine ARC photometry, DIS spectra, and Gemini spectra to mass-model the system. They find the broadband colors are not consistent with a catastrophic formation, but are best fit by exponentially declining SFH. They think the main difference between Malin 2 and non-giant LSB galaxies is the dark matter halo scale. I think this is begging the question a little bit

Pickering et al. (1997) has the H I rotation curves of these guys. For UGC 6614, has M H I $= 2.5 \pm 0.2 \times 10^{10} M_{\odot} h_{75}^{-2}$. And $3.6 \pm 0.4 \times 10^{10} M_{\odot} h_{75}^{-2}$for Malin 2. Notes that these are galaxies that are massive and DM dominated. In Malin 2, they find some gas moving relative to the regular rotating disk, and suspect that a dwarf fell though and stimulated star formation and this could be how stars managed to form in the low density environment.

Can we say that the stars formed in a higher density environment and then got dispersed.

Das (2013) look at the environments of GLSB systems. He says that GLSBs are an extreme form of late type spiral galaxies. I think I can show that no, they are really normal elliptical galaxies that happen to have accreted disks.

Standard catalogs list these systems as Sd and Sa galaxies, so they are commonly thought of as spirals.

Nice paper on galaxies that live in voids and how one did manage to build a polar H I disk with no stars: Stanonik et al. (2009)

Chemical abundances in a polar disk: Spavone et al. (2010)

a near scoop by Lelli et al. (2010). They re-analyze H I data on Malin 1 and one other. But a nice place to look for introduction material. They point out that GLSB galaxies might be normal HSB galaxies in the center. They claim to see steeply rising rotation curves, and compare to formation mechanisms.

Morganti et al. (1997) look at an elliptical with an H I disk. Find a nice flat rotation curve. Emonts et al. (2008) Another massive H I ring around an S0 galaxy. Weijmans et al. (2008) another H I ring around an early type. Anne-Marie has lots of SAURON papers pushing out to large radii in ellipticals.

Barth (2007) analyze HST imaging of Malin 1 and find that the central object is well described as a normal SB0/a galaxy. Makes good point that lots of the other large disk observations look like they are extensions of the inner galaxy, while Malin 1's disk is probably a distinct component.

Peñarrubia et al. (2006) look at forming extended disks by disrupting a dwarf galaxy.

Ibata et al. (2005) look at extended disk of M31.

Ibata et al. (2013) claim M31 satellites are co-planer.

McConnachie et al. (2009) M31 survey showing lots of merger structure.

Bothun of course has a nice web page with images at: http://zebu.uoregon.edu/sb2.html

another nice image at http://www.capella-observatory.com/ImageHTMLs/Galaxies/UGC6614.htm

From Matthews et al. (2001), H I measurements on the gals: Matthews et al. (2001) also lists some incs values–calls Malin2 an Scd/Sd galaxy, has some good tables that are only available on-line. I'll need to compare my stellar kinematics to the H I kinematics.

Rahman et al. (2007) has Spitzer observations of a few GLSB galaxies.

Das et al. (2010) find CO in Malin 2. Make some points about it being stable

Mapelli & Mayer (2012) making ring galaxies from off center collisions.

Mapelli et al. (2008) look at if ring galaxies could evolve into GLSB systems.

Schiminovich et al. (2013): Observe H I shells in ellipticals.

Iodice et al. (2006): Nice minor and major axis observation of a polar-ring galaxy.

Brook et al. (2008): Makes a polar ring galaxy via extended accretion of cosmological gas. They say polar disk galaxies are built just like the outskirts of regular galaxies, they just happen to be very mis-aligned.

Schweizer et al. (1989) Do a similar study with IC 2006, where they observe an H I ring around the elliptical galaxy to get the total mass at large radii. Looks like they get out to about 12.5 kpc.

Oosterloo et al. (2007) HIPASS detection of H I gas around 30 early-type galaxies. Most have regular disk or ring kinematics. Suggest these are ancient. They don't seem to have the resolution to do in-depth kinematics and DM halo stuff.

Magain & Chantry (2013) look at strong lenses around 25 ellipticals, and then claim they see no evidence for extended DM halos. Confusing plot–Maybe they get out to 5 $R_{1/2}$? They say they only need a factor of 2, that could come from baryonic dark matter.

Sprayberry et al. (1995) CCD imaging of 8 GLSB systems.

Morganti et al. (2013) Do modeling of ellipticals with declining velocity dispersion profiles. Good place to start looking for the best way to model the long-slit data.

Buote & Humphrey (2012) review of dark matter in ellipticals from x-ray observations.

XXX-clearly need to look up bulge-to-disk metallicity gradient. Lauren did it with colors in MacArthur et al. (2004). Nice look with metallicity gradients as a function of scale-length, and kpc, and vrot and galaxy type. Did spectra gradients in MacArthur et al. (2009). MANGA would make this easy to compare...Maybe there's a SAURON paper on metallicity gradients.

XXX-need to look up some Thilker papers on extended UV disks, since these objects could be similar. From his talk, UGC 1382 shows up in stripe 82 coadd (and NUV). UGC 3642, GALEX shows a disk, and H I is counter rotating.

Salim & Rich (2010) Looks at HST imaging of z = 0.1 early type galaxies that have UV excess, and finds some extended disks. They think the gas and star formation is comming from minor mergers or accretion.

Salim et al. (2012) Finds 2 more GLSB type objects – could be a sign that there are multiple routes to making GLSB systems.

The other way to measure the dark matter halo of an elliptical is to use gravitational lensing. Belokurov et al. (2007) find a large ring in SDSS.

Table 1. Basic Properties of GLSB Galaxies

Name	SDSS ID (DR 9)	z	r (mag)	R_e arcsec	σ km s^{-1}	Stellar Mass $\log_{10}M_\odot$	H I mass $\log_{10}M_\odot$
Malin 2	1237667735572381852	0.046	14.34	7.17	202	11.15	10.6
UGC 06614	1237668585435365393	0.021	13.52	7.3	150	10.66	10.5

Note. — H I masses updated to our adopted cosmological parameters from Pickering et al. (1997). The rest taken from SDSS.

Table 2. Fitted Structural Properties

Name	h_r (arcsec)	inclination (deg)
Malin 2	6.1	35.5
UGC 06614	5.7	33.4

2. Observations

2.1. IFU spectra

We obtained spatially resolved spectroscopy of our target galaxies using the Mitchell Spectrograph (formerly VIRUS-P)(Hill et al. 2008) on the 2.7m Harlan J. Smith telescope at McDonald Observatory. Observations were made during dark time in February, March, and April 2010. Identical instrument setups were used for all observations. The Mitchell Spectrograph with the VP-2 IFU bundle used here has a square array of 246 optical fibers which sample the $1.9' \times 1.9'$ field-of-view with a 1/3 filling factor, with each fiber having a diameter of $4.23''$. The spectrograph images the spectrum of each fiber on a 2048×2048 Fairchild Imaging CCD.

For each galaxy, observations were taken at three unique dither positions to provide nearly complete spatial coverage. Individual science exposures were 30 minutes. Malin 2 had 10 exposures per dither position (11 exposures for dither position 1), for a total of 15 hours of exposure time. Observations of UGC 06614 had alignment issues between observing runs. This resulted in a deep stack of 6 exposures, and a shallow stack with only 2 exposures. With only 2 exposures, cosmic ray rejection becomes difficult, therefore, we use these shallow frames when looking at the surface brightness profiles, but use only the aligned deep co-add when analyzing the stellar kinematics and stellar populations. Twilight flat field frames, bias frames, and wavelength calibration Hg and Cd lamps were taken during the day. Flux standard stars were observed in twilight.

We use the Mitchell Spectrograph software pipeline Vaccine (Adams et al. 2011) to perform basic reduction tasks. Vaccine subtracts the over-scan region and generates and subtracts a bias frame. Bad pixels are masked. Twilight flats and arc lamps from each night are combined. The combined flat frame is used to trace the spatial profile of each fiber and correct for pixel-to-pixel variation. The combined arc lamp is used to fit a wavelength solution for each fiber. We use a 4th order polynomial and find the wavelength solutions have a typical RMS of 0.06-0.2 Å ($\sim$ 0.1 pixel). Vaccine then masks potential cosmic rays and collapses each fiber to a one dimensional spectrum. The fibers are adequately spaced, and our targets are predominately low surface brightness, so we find making a fiber cross-talk correction unnecessary.

Once the Vaccine routines are completed we make the following additional reductions using standard IRAF routines and custom IDL scripts. The reduced twilight frames are used to generate a fiber-to-fiber flux correction (similar to a longslit illumination correction). We use the b-spline procedure described in Kelson (2003) to generate background frames. The corners of each frame contain enough empty fibers to measure the sky background in each

exposure. Because we bin fibers together, imperfect sky-subtraction represents a serious source of potential systematic errors.

The spectra are then rectified to a common wavelength scale, and the photo-spectroscopic standards are used to flux calibrate the spectra and correct for atmospheric extinction. The spectra are then velocity shifted to the Local Standard of Rest. Images taken at identical dither positions are averaged together with outlier rejection to eliminate any remaining cosmic rays. Some observations were taken in non-photometric conditions, so before combining frames we scale them to a common average flux level.

Our final reduced data for each galaxy includes 738 spectra spanning a $1.9' \times 1.9'$ field-of-view. The spectra have a wavelength range of ∼3550-5840 with 2.2 Å pixels (with some fibers only reaching 5500 Å due to the warping of the trace). The FWHM of reduced arc lamp images is 5.3 Å, giving us a resolution of $R \sim 700 - 1000$. The fiber-to-fiber changes in resolution are less than 10%.

With our final reduced data cubes, we used Penalized Pixel-Fitting (pPXF) (Cappellari & Emsellem 2004) and Gas AND Absorption Line Fitting (GANDALF) (Sarzi et al. 2006) on each fiber to fit stellar velocities, stellar dispersions, and emission line velocities and fluxes. For stellar templates we use a suite of SSP spectra from Bruzual & Charlot (2003). We use GANDALF to measure the [O II] doublet, [O III] doublet, and the higher order Balmer lines Hβ, Hγ, Hδ, Hϵ while masking the night skyline at 5577 Å. The fit also includes a 4th degree multiplicative polynomial to correct for any dust or flux calibration mis-match between the observations and templates. Because our data do not extend out to Hα, we cannot use the Balmer decrement to place tight constraints on the dust extinction. While pPXF fits the stellar velocity dispersion, our instrumental resolution is low enough (~ 140 km s^{-1}) that we are unable to make meaningful velocity dispersion measurements beyond the central fibers.

In addition to individual fibers, we have binned neighboring fibers together to boost the signal-to-noise ratio and run pPXF on these super-fibers.

3. Comparisons to Other Galaxies

By eye, GLSB systems resemble large faint spiral disks at large radii, and regular ellipticals at their centers. In the SDSS DR10 (Ahn et al. 2014), the Galaxy Zoo classifications (Willett et al. 2013) are spiral for Malin 1 and 2 and UGC 6614. In this section, we compare the properties of the GLSB centers and disks with other systems.

3.1. GLSB Centers

Both our objects have been observed with SDSS, making it possible to compare them to a large number of systems. The outer disks of GLSBs are faint enough that the SDSS photometric pipeline effectively ignores them.

To make a comparison sample of galaxies from SDSS, we select galaxies with redshifts between 0.01 and 0.07 and de-reddned r magnitude between 13.5 and 17.7. When comparing to just elliptical galaxies we make the additional color-cut of $u - r > 2.1$ (and some morphology selectors). These are simply galaxies for comparison, not a rigorously defined volume-complete sample. Our full SQL querries are shown in §A. This gives us a sample of 141,001 objects, 45,703 of which have red colors. Throughout, we use the CosmoloPy[1] fiducial cosmology ($h = 0.704$, $\Omega_{m_0} = 0.2726$, $\Omega_{\lambda_0} = 0.7274$).

Figure 1 shows where the GLSBs fall on the major galaxy relations. We use extinction corrected magnitudes and k-corrected colors(Chilingarian et al. 2010). Both of our GLSBs lie on the red-sequence in a color-magnitude diagram.

The central regions of GLSBs are often called "bulges", however, looking at Figure 1, it is clear that these are much brighter than bulges of typical spiral galaxies and the GLSBs are on the bright end of the red-sequence.

We follow Bernardi et al. (2003a,b) in fitting fundamental plane parameters to our selected SDSS galaxies. We fit the fundamental plane by minimizing χ^2 in,

$$\chi^2 = \log R_0 - a \log \sigma - b \log I_0 - c \tag{1}$$

where R_0 is the effective radius, σ is velocity dispersion in kilometers per second and I_0 is the surface brightness. The resulting best-fit parameters are a =1.376 , b = -0.661, c = -9.938. We note that we have not made a rigorous volume-complete selection of galaxies, rather, simply galaxies with similar magnitudes, colors, and redshifts to our GLSBs. See Saulder et al. (2013) for a more rigorous analysis of the Fundamental Plane in SDSS.

3.2. GLSB Disks

The diameters of these disks are very large. Stellar disks are typically embedded in much larger H I disks. The size of the GLSB stellar disks is similar to the largest H I disks observed in nearby galaxies, in support of the Mapelli et al. (2008) model where the GLSB

[1] `http://roban.github.com/CosmoloPy/`

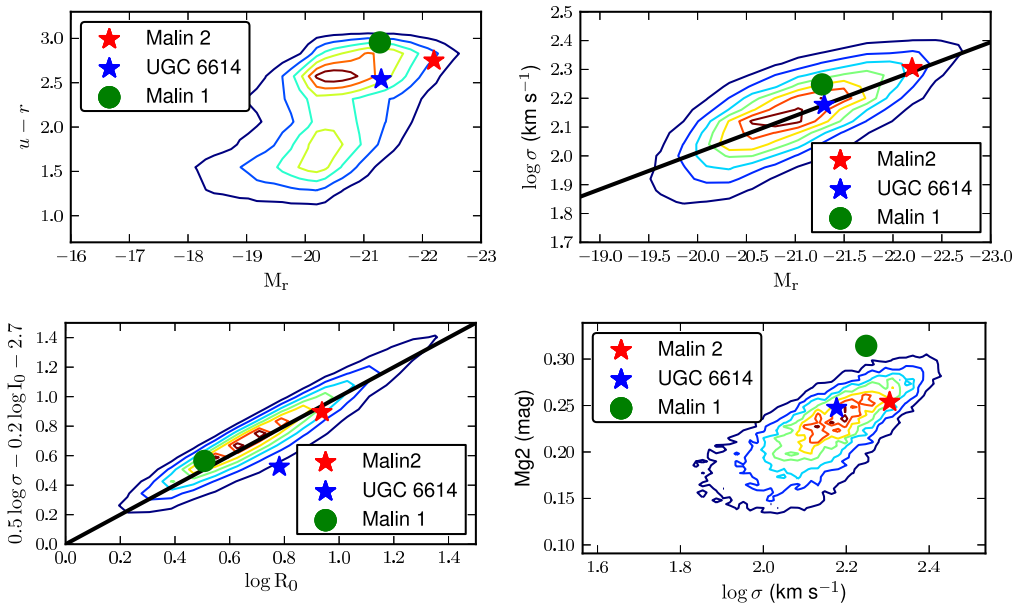

Fig. 1.— Top Left: The color-magnitude diagram for 141,000 galaxies of similar redshift and magnitude as Malin 2 and UGC 6614. Top Right: The Faber-Jackson relation for 45,700 SDSS galaxies, along with a best-fit line. Left: The r-band Fundamental Plane from SDSS along with our GLSB galaxies and best-fit line. Bottom Right: The relation between central velocity dispersion and the Mg2 absorption feature. Looking at the SDSS data, our GLSB galaxies appear as normal red elliptical galaxies.

disks are the faded remnants of a normal H I disk that has experienced a merger induced star-burst.

For comparison: Williams et al. (2013) trace star formation out to 11 disk scale lengths (radius of 22 kpc) in NGC 2403. Maybe also look at THINGS data for comparisons on how large galaxy disks get.

Papers that have large H I rotation curves that I might compare to: de Blok et al. (2008); Swaters et al. (2009); Verheijen (2001)

In Figure 2, we compare the sizes of the stellar disks of the GLSB galaxies with other observations. For this plot, we take the maximum detected radius from the literature for the galaxies. It is possible that deeper observations could increase the values of R_{max}. While UGC 6614 close in size to the upper end of local H I disks, Malin 1 and 2 are much larger than galaxies observed in the THINGS survey. This seems to point against the GLSB formation mechanism of Mapelli et al. (2008), as we do not observe H I disks large enough to convert into GLSB systems without some additional source of angular momentum.

4. Kinematics

It might be nice to spin this as a chance to measure the DM halo of ellipticals to very large radii. Some relevant papers for comparison: Weijmans et al. (2009) use SAURON to get way out. Proctor et al. (2009) use Keck. Murphy et al. (2011) use VP.

The kinematics of the extended GLSB disks represents a unique probe for measuring the extended dark matter halo of elliptical galaxies.

We use the kinemetry package presented in Krajnović et al. (2006) to fit a tilted-ring model to the stellar kinematics. For these fits, we hold the position angle and inclination fixed to values found from fitting the fiber-photometry. Figures 5 and 13 show the kinemetry fits and extracted rotation curves. We iterate the fit, clipping residuals which deviate from the model my more than 250 km s^{-1}.

While we are making rather sweeping assumptions about the nature of the GLSB disks by fitting a simple disk with fixed position angle and inclination, the fits are quite good. We also note that by observing disks, we do not have to worry about the velocity anisotropy parameter that traditionally makes dynamical modeling of ellipticals difficult.

Notes on individual rotation curves: The Malin 2 rotation curve is rather complicated, having several abrupt rises. This is especially strange given the very smooth photometric

profile. UGC 6614, on the other hand, has a relatively normal spiral galaxy-like rotation curve that rises linearly out to 10 kpc and then flattens.

The lack of rotation in the central regions of the galaxies is not particularly surprising, as this is the region that is flux-dominated by the central elliptical galaxy. XXX-that hopefully we have data that shows they are not rotating or rotating in a different orientation.

The extracted rotation curves imply large dark matter halos. For Malin 2, $V_{circ} \sim 280$ km s^{-1}at $R = 42$ kpc implies a mass of 7.6×10^{11}M$_\odot$ (compared to an SDSS stellar mass of 1.4×10^{11}). For UGC 6614, $V_{circ} \sim 200$ km s^{-1}at $R = 17$ kpc gives a dynamical mass of 1.6×10^{11}M$_\odot$ (compared to a stellar mass of0.46×10^{11}M$_\odot$).

If we use the circular speed of the H I data, we end up with masses of 25×10^{11}M$_\odot$ for Malin 2 and 6.5×10^{11}M$_\odot$ for UGC 6614. So that's dynamical to stellar mass ratios of 18 and 14 respectively. Looks like they both have M$_{\rm HI}$ around 3-4 10^{10}M$_\odot$.

Thus, for Malin 2, we reach a radius of $\sim 6.2R_e$, and find a dark matter fraction of 81%. For UGC 6614, we reach a radius of $\sim 5.2R_e$ and find a dark matter fraction of 71%.

Murphy et al. (2011) reach $\sim 2R_e$ using just stellar data, and then rely on globular cluster kinematics to extended out to $5R_e$.

XXX-crap, whatever happened to the gas kinematics? There are emission lines out there–are they bright enough to get in single fibers of not? Looks like for Malin 2 the emission lines are only coming from one side of the galaxy. UGC 6614 is mostly emission from the center.

XXX-It would be great to get high resolution H I observations of these systems since they could probably be higher spatial resolution.

5. Star Formation Histories

Following the work in Yoachim et al. (2010, 2012), we generate a suite of model galaxy SEDs using relatively simple star formation histories and find the best fitting single model. We break the star formation history into three age bins, 0-10 Gyr, 10-11.5 Gyr, and 11.5-12 Gyr. We assume each age bin has a constant star formation with a level of 0, 0.5, 1, or 10 solar-masses per year. Each SFH can have a metallicity of [Z/H] = -2.3,-1.70,-0.70, -0.40, 0.0, or 0.40. We do not include any metallicity evolution, as all the age bins in a given model has the same metallicity. This gives us 361 unique non-zero model spectra.

Figures 6 and 10 show the fibers that were binned and the resulting spectra for Malin

2 and UGC 06614. Both galaxies have elliptical-galaxy like spectra in their centers, with outskirts that have significant emission lines.

The best fitting star formation histories are shown in Figures 7 and 11, while the best fitting stellar metallicities are shown in Figures 8 and 12. We find that *both galaxies have stellar populations dominated by old stars at all radii*. While the outer disks have emission lines and have spectra that are best fit with some current star formation, the total stellar mass is still overwhelmingly dominated by old stars. Both galaxies also show very steep metallicity gradients, with centers that are super-solar metallicity (at the limit of our models), while the outer disks are both best fit by [Z/H]=-0.7.

A problem with fitting observed galaxy spetra with templates is that residuals between the model and data are dominated by non-Gaussian systematic effects such as template mis-match and improper parameterization of the SFH. Since the residuals are non-Guassian, there is no statistical formalism for generating uncertanties in the fit. To generate our error bars, we look at the range of fits which have χ^2 values within 100 of the minimum. In many cases, this eliminates nearly all fits except for the minimum. In these cases, we use the 4 best-fitting models to estimate the range of possible fits.

The dominance of an old stellar population at large radii seems to contradict the starburst formation mechanism of Mapelli et al. (2008), and favor an accretion model where a galaxy already containing old stars is disrupted by a massive elliptical galaxy.

These are incredibly steep metallicity gradients. The logarithmic gradients δ[Z/H] $\log \mathrm{R/R_e}$ is ~ -1.6 for Malin 2 and ~ -0.68 for UGC 6614. These are very steep compared to gradients typically observed in elliptical galaxies (Greene et al. 2012). Other cites for elliptical gradients (Kuntschner et al. 2010)

6. Disk Progenitors

It should be relatively easy to speculate about the galaxies that merged to form the disk. I can pull H I masses, and then calc some stellar masses given the SDSS photometry and my own stellar M/L ratios. Then given a baryonic mass and a typical stellar metallicity, it should be easy match that up to something. Using baryonic TF relation, I'm getting pretty large V_c values for what the accreted galaxy would have been. I guess we could even speculate that this was a 3+ body encounter, so multiple gas rich systems that settle in. That would help explain the low metallicities.

Figure 3 shows the total H I mass for galaxies observed in the THINGS survey (Walter

et al. 2008), along with the H I masses for GLSB galaxies (Pickering et al. 1997).

We can't really use the stellar luminosity of the disk to constrian the projenitor since there are signs of current *i*n situ star formation in the disks. However, the very low stellar metalicities point to low-mass projenitors.

Hard to estimate what the progenitor system of the disks were. Is there a good plot of disk H I mass and metallicity out there? Might even need to measure Lick indices to try and get everything on the same metallicity system.

These systems are rare enough, that one might imagine rather complicated scenarios for creating them. For example, a three-body enocounter could eject one galaxy while leaving a second in a nearly circular orbit. Back of the envelope, a galaxy ejected at 5000 km s^{-1}would go 1.5 degrees per gigayear. Even if the ejection was partly along the line of sight, it would be hard to find several gigayears later. Unlike the collisional ring scenario where one would expect the galaxy that stimulated the ring formation to still be nearby.

The basic observational properties of GLSBs that need to be explained:

1. These galaxies have H I disks that extend much farther than typical spiral galaxies (Figure 2).
2. While GLSBs have large disks, the total H I mass in these disks is lower than expected given their rotational velocities (Figure 3)
3. The central bulges are similar to elliptical galaxies in SDSS (Figure 1).
4. The stellar populations in the centers of GLSBs are old and very metal rich.
5. The stellar populations in the extended disks shows some signs of ongoing star formation, but is consistent with being dominated by an old metal poor population.

7. Discussion

We find that the centers of these two GLSB systems very closely resemble normal galaxies, with the extended faint disks being distinct components, in line with the previous results for Malin 1 (Barth 2007) and NGC 7589 (Lelli et al. 2010).

An accretion formation scenario does the best job explaining all the observations. While a collisional ring could fade to a GLSB, the stellar population should be relatively young,

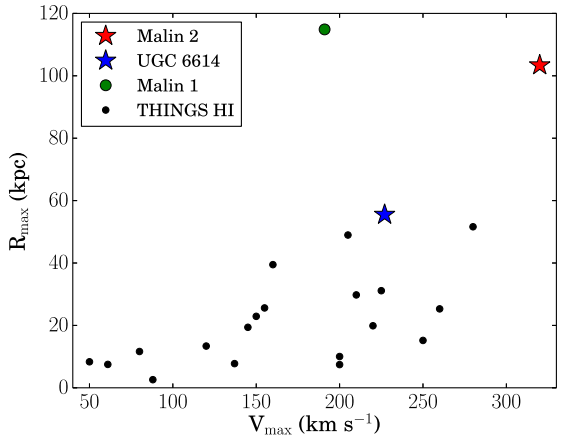

Fig. 2.— Comparison of the GLSB disks with other galaxy disks from the literature. THINGS data taken from de Blok et al. (2008), Malin 1 from Moore & Parker (2006), Malin 2 and UGC 6614 from Pickering et al. (1997). Here, R_{max} is the maximum radius with an H I detection. It is interesing to note that the stellar disks of GLSB galaxies are often larger than the H I disks of nearby systems.

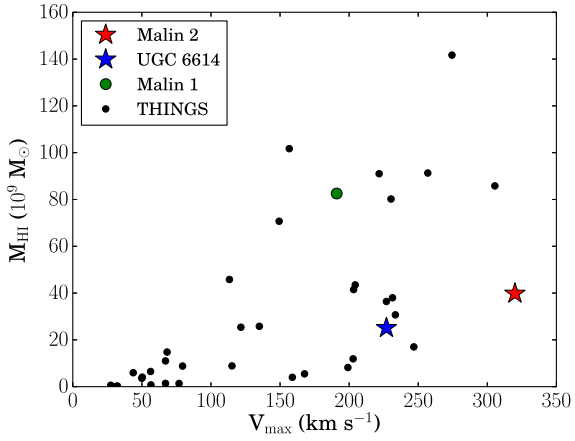

Fig. 3.— Comparison of GLSB H I masses with H I masses measured in the THINGS survey (Walter et al. 2008). While the H I masses in the GLSB systems are high, they are consistent with what would be available in a merger with a ∼110 km/s galaxy, assuming the merger did not trigger large amounts of star formation and feedback.

and one might not expect a steep metallicity gradient. Also, there are no obvious galaxies near GLSBs to act as progenitor colliders.

It also seems unlikely that GLSBs are just extreme versions of normal disk galaxies (Das 2013). It's hard to imagine how such a large massive central spheroid could be formed without also disrupting the surrounding disk.

Accretion can also form GLSB systems around any type of host galaxy, explaining how Barth (2007) can find that Malin 1 is an SB0 galaxy, while our two systems are normal ellipticals.

Our initial long slit observations don't really show much as far as correlation between the bulge and disk rotation vectors. We are currently proposing for higher resolution observations that will make it possible to measure the stellar kinematics of the central object in detail to see if it is a relatively undisturbed elliptical.

If these systems do prove to be ellipticals with accreted high angular momentum disks, they represent an amazing opportunity to probe the dark matter halo properties of elliptical systems to very large radii.

Should probably figure out if these things are fast or slow rotators by the Emsellem et al. (2011) definition. Also see Cappellari et al. (2011) that says slow rotators are very rare in the field. So it might be strange if Malin 2 and UGC 6614 are slow rotators...

8. Conclusions

We have observed two giant low surface brightness galaxies with the VIRUS-P IFU. We find the systems are best explained as massive elliptical galaxies which have managed to accrete stars and gas into a lareg disk. The stellar stars have a disk-like velocity field, and are dominated by old stars, but do show signs of ongoing star formation.

In a future work, we plan to combine our IFU observations with higher spatial resolution long-slit specta from the Apache Point 3.5m telescope to determine if the central ellipticals are dynamically distinct from their disks. This data will also help up build dynamicall models for the systems.

Thanks to Dave Doss and the staff at McDonald Observatory for their help on these observing runs. Thanks to the observing specialists at Apache Point for their help executing our remote observations.

This paper includes data taken at The McDonald Observatory of The University of Texas at Austin.

Based on observations obtained with the Apache Point Observatory 3.5-meter telescope, which is owned and operated by the Astrophysical Research Consortium.

This research made use of the "K-corrections calculator" service available at http://kcor.sai.msu.ru/

GANDALF was developed by the SAURON team and is available from the SAURON website (www.strw.leidenuniv.nl/sauron). See also Sarzi et al. (2006, MNRAS, 366, 1151) for details.

Funding for SDSS-III has been provided by the Alfred P. Sloan Foundation, the Participating Institutions, the National Science Foundation, and the U.S. Department of Energy Office of Science. The SDSS-III web site is http://www.sdss3.org/.

SDSS-III is managed by the Astrophysical Research Consortium for the Participating Institutions of the SDSS-III Collaboration including the University of Arizona, the Brazilian Participation Group, Brookhaven National Laboratory, University of Cambridge, Carnegie Mellon University, University of Florida, the French Participation Group, the German Participation Group, Harvard University, the Instituto de Astrofisica de Canarias, the Michigan State/Notre Dame/JINA Participation Group, Johns Hopkins University, Lawrence Berkeley National Laboratory, Max Planck Institute for Astrophysics, Max Planck Institute for Extraterrestrial Physics, New Mexico State University, New York University, Ohio State University, Pennsylvania State University, University of Portsmouth, Princeton University, the Spanish Participation Group, University of Tokyo, University of Utah, Vanderbilt University, University of Virginia, University of Washington, and Yale University.

REFERENCES

Adams, J. J., Blanc, G. A., Hill, G. J., Gebhardt, K., Drory, N., Hao, L., Bender, R., Byun, J., Ciardullo, R., Cornell, M. E., Finkelstein, S. L., Fry, A., Gawiser, E., Gronwall, C., Hopp, U., Jeong, D., Kelz, A., Kelzenberg, R., Komatsu, E., MacQueen, P. J., Murphy, J., Odoms, P. S., Roth, M., Schneider, D. P., Tufts, J. R., & Wilkinson, C. P. 2011, ApJS, 192, 5

Ahn, C. P., Alexandroff, R., Allende Prieto, C., Anders, F., Anderson, S. F., Anderton, T., Andrews, B. H., Aubourg, É., Bailey, S., Bastien, F. A., & et al. 2014, ApJS, 211, 17

Barth, A. J. 2007, AJ, 133, 1085

Belokurov, V., Evans, N. W., Moiseev, A., King, L. J., Hewett, P. C., Pettini, M., Wyrzykowski, L., McMahon, R. G., Smith, M. C., Gilmore, G., Sanchez, S. F., Udalski, A., Koposov, S., Zucker, D. B., & Walcher, C. J. 2007, ApJ, 671, L9

Bernardi, M., Sheth, R. K., Annis, J., Burles, S., Eisenstein, D. J., Finkbeiner, D. P., Hogg, D. W., Lupton, R. H., Schlegel, D. J., SubbaRao, M., Bahcall, N. A., Blakeslee, J. P., Brinkmann, J., Castander, F. J., Connolly, A. J., Csabai, I., Doi, M., Fukugita, M., Frieman, J., Heckman, T., Hennessy, G. S., Ivezić, Ž., Knapp, G. R., Lamb, D. Q., McKay, T., Munn, J. A., Nichol, R., Okamura, S., Schneider, D. P., Thakar, A. R., & York, D. G. 2003a, AJ, 125, 1817

—. 2003b, AJ, 125, 1866

Bothun, G. D., Impey, C. D., Malin, D. F., & Mould, J. R. 1987, AJ, 94, 23

Brook, C. B., Governato, F., Quinn, T., Wadsley, J., Brooks, A. M., Willman, B., Stilp, A., & Jonsson, P. 2008, ApJ, 689, 678

Bruzual, G., & Charlot, S. 2003, MNRAS, 344, 1000

Buote, D. A., & Humphrey, P. J. 2012, in Astrophysics and Space Science Library, Vol. 378, Astrophysics and Space Science Library, ed. D.-W. Kim & S. Pellegrini, 235

Cappellari, M., & Emsellem, E. 2004, PASP, 116, 138

Cappellari, M., Emsellem, E., Krajnović, D., McDermid, R. M., Serra, P., Alatalo, K., Blitz, L., Bois, M., Bournaud, F., Bureau, M., Davies, R. L., Davis, T. A., de Zeeuw, P. T., Khochfar, S., Kuntschner, H., Lablanche, P.-Y., Morganti, R., Naab, T., Oosterloo, T., Sarzi, M., Scott, N., Weijmans, A.-M., & Young, L. M. 2011, MNRAS, 416, 1680

Chilingarian, I. V., Melchior, A.-L., & Zolotukhin, I. Y. 2010, MNRAS, 405, 1409

Das, M. 2013, Journal of Astrophysics and Astronomy, 34, 19

Das, M., Boone, F., & Viallefond, F. 2010, A&A, 523, A63

de Blok, W. J. G., Walter, F., Brinks, E., Trachternach, C., Oh, S.-H., & Kennicutt, Jr., R. C. 2008, AJ, 136, 2648

Dutton, A. A., & van den Bosch, F. C. 2012, MNRAS, 421, 608

Emonts, B. H. C., Morganti, R., Oosterloo, T. A., Holt, J., Tadhunter, C. N., van der Hulst, J. M., Ojha, R., & Sadler, E. M. 2008, MNRAS, 387, 197

Emsellem, E., Cappellari, M., Krajnović, D., Alatalo, K., Blitz, L., Bois, M., Bournaud, F., Bureau, M., Davies, R. L., Davis, T. A., de Zeeuw, P. T., Khochfar, S., Kuntschner, H., Lablanche, P.-Y., McDermid, R. M., Morganti, R., Naab, T., Oosterloo, T., Sarzi, M., Scott, N., Serra, P., van de Ven, G., Weijmans, A.-M., & Young, L. M. 2011, MNRAS, 414, 888

Greene, J. E., Murphy, J. D., Comerford, J. M., Gebhardt, K., & Adams, J. J. 2012, ApJ, 750, 32

Hill, G. J., MacQueen, P. J., Smith, M. P., Tufts, J. R., Roth, M. M., Kelz, A., Adams, J. J., Drory, N., Grupp, F., Barnes, S. I., Blanc, G. A., Murphy, J. D., Altmann, W., Wesley, G. L., Segura, P. R., Good, J. M., Booth, J. A., Bauer, S., Popow, E., Goertz, J. A., Edmonston, R. D., & Wilkinson, C. P. 2008, SPIE, 7014

Ibata, R., Chapman, S., Ferguson, A. M. N., Lewis, G., Irwin, M., & Tanvir, N. 2005, ApJ, 634, 287

Ibata, R. A., Lewis, G. F., Conn, A. R., Irwin, M. J., McConnachie, A. W., Chapman, S. C., Collins, M. L., Fardal, M., Ferguson, A. M. N., Ibata, N. G., Mackey, A. D., Martin, N. F., Navarro, J., Rich, R. M., Valls-Gabaud, D., & Widrow, L. M. 2013, Nature, 493, 62

Iodice, E., Arnaboldi, M., Saglia, R. P., Sparke, L. S., Gerhard, O., Gallagher, J. S., Combes, F., Bournaud, F., Capaccioli, M., & Freeman, K. C. 2006, ApJ, 643, 200

Kasparova, A. V., Saburova, A. S., Katkov, I. Y., Chilingarian, I. V., & Bizyaev, D. V. 2014, MNRAS, 437, 3072

Kelson, D. D. 2003, PASP, 115, 688

Krajnović, D., Cappellari, M., de Zeeuw, P. T., & Copin, Y. 2006, MNRAS, 366, 787

Kuntschner, H., Emsellem, E., Bacon, R., Cappellari, M., Davies, R. L., de Zeeuw, P. T., Falcón-Barroso, J., Krajnović, D., McDermid, R. M., Peletier, R. F., Sarzi, M., Shapiro, K. L., van den Bosch, R. C. E., & van de Ven, G. 2010, MNRAS, 408, 97

Lelli, F., Fraternali, F., & Sancisi, R. 2010, A&A, 516, A11+

MacArthur, L. A., Courteau, S., Bell, E., & Holtzman, J. A. 2004, ApJS, 152, 175

MacArthur, L. A., González, J. J., & Courteau, S. 2009, MNRAS, 395, 28

Magain, P., & Chantry, V. 2013, ArXiv e-prints

Mapelli, M., & Mayer, L. 2012, MNRAS, 420, 1158

Mapelli, M., Moore, B., Ripamonti, E., Mayer, L., Colpi, M., & Giordano, L. 2008, MNRAS, 383, 1223

Matthews, L. D., van Driel, W., & Monnier-Ragaigne, D. 2001, A&A, 365, 1

McConnachie, A. W., Irwin, M. J., Ibata, R. A., Dubinski, J., Widrow, L. M., Martin, N. F., Côté, P., Dotter, A. L., Navarro, J. F., Ferguson, A. M. N., Puzia, T. H., Lewis, G. F., Babul, A., Barmby, P., Bienaymé, O., Chapman, S. C., Cockcroft, R., Collins, M. L. M., Fardal, M. A., Harris, W. E., Huxor, A., Mackey, A. D., Peñarrubia, J., Rich, R. M., Richer, H. B., Siebert, A., Tanvir, N., Valls-Gabaud, D., & Venn, K. A. 2009, Nature, 461, 66

Moore, L., & Parker, Q. A. 2006, Publications of the Astronomical Society of Australia, 23, 165

Morganti, L., Gerhard, O., Coccato, L., Martinez-Valpuesta, I., & Arnaboldi, M. 2013, MNRAS, 431, 3570

Morganti, R., Sadler, E. M., Oosterloo, T., Pizzella, A., & Bertola, F. 1997, AJ, 113, 937

Murphy, J. D., Gebhardt, K., & Adams, J. J. 2011, ApJ, 729, 129

Oosterloo, T. A., Morganti, R., Sadler, E. M., van der Hulst, T., & Serra, P. 2007, A&A, 465, 787

Peñarrubia, J., McConnachie, A., & Babul, A. 2006, ApJ, 650, L33

Pickering, T. E., Impey, C. D., van Gorkom, J. H., & Bothun, G. D. 1997, AJ, 114, 1858

Proctor, R. N., Forbes, D. A., Romanowsky, A. J., Brodie, J. P., Strader, J., Spolaor, M., Mendel, J. T., & Spitler, L. 2009, MNRAS, 398, 91

Rahman, N., Howell, J. H., Helou, G., Mazzarella, J. M., & Buckalew, B. 2007, ApJ, 663, 908

Raskutti, S., Greene, J. E., & Murphy, J. D. 2014, ApJ, 786, 23

Salim, S., Fang, J. J., Rich, R. M., Faber, S. M., & Thilker, D. A. 2012, ApJ, 755, 105

Salim, S., & Rich, R. M. 2010, ApJ, 714, L290

Sarzi, M., Falcón-Barroso, J., Davies, R. L., Bacon, R., Bureau, M., Cappellari, M., de Zeeuw, P. T., Emsellem, E., Fathi, K., Krajnović, D., Kuntschner, H., McDermid, R. M., & Peletier, R. F. 2006, MNRAS, 366, 1151

Saulder, C., Mieske, S., Zeilinger, W. W., & Chilingarian, I. 2013, A&A, 557, A21

Schiminovich, D., van Gorkom, J. H., & van der Hulst, J. M. 2013, AJ, 145, 34

Schweizer, F., van Gorkom, J. H., & Seitzer, P. 1989, ApJ, 338, 770

Spavone, M., Iodice, E., Arnaboldi, M., Gerhard, O., Saglia, R., & Longo, G. 2010, ArXiv e-prints

Sprayberry, D., Impey, C. D., Bothun, G. D., & Irwin, M. J. 1995, AJ, 109, 558

Stanonik, K., Platen, E., Aragon-Calvo, M. A., van Gorkom, J. H., van de Weygaert, R., van der Hulst, J. M., Kovac, K., Yip, C. ., & Peebles, P. J. E. 2009, ArXiv e-prints

Swaters, R. A., Sancisi, R., van Albada, T. S., & van der Hulst, J. M. 2009, A&A, 493, 871

Verheijen, M. A. W. 2001, ApJ, 563, 694

Walter, F., Brinks, E., de Blok, W. J. G., Bigiel, F., Kennicutt, Jr., R. C., Thornley, M. D., & Leroy, A. 2008, AJ, 136, 2563

Weijmans, A.-M., Cappellari, M., Bacon, R., de Zeeuw, P. T., Emsellem, E., Falcón-Barroso, J., Kuntschner, H., McDermid, R. M., van den Bosch, R. C. E., & van de Ven, G. 2009, MNRAS, 398, 561

Weijmans, A.-M., Krajnović, D., van de Ven, G., Oosterloo, T. A., Morganti, R., & de Zeeuw, P. T. 2008, MNRAS, 383, 1343

Willett, K. W., Lintott, C. J., Bamford, S. P., Masters, K. L., Simmons, B. D., Casteels, K. R. V., Edmondson, E. M., Fortson, L. F., Kaviraj, S., Keel, W. C., Melvin, T., Nichol, R. C., Raddick, M. J., Schawinski, K., Simpson, R. J., Skibba, R. A., Smith, A. M., & Thomas, D. 2013, MNRAS, 435, 2835

Williams, B. F., Dalcanton, J. J., Stilp, A., Dolphin, A., Skillman, E. D., & Radburn-Smith, D. 2013, ApJ, 765, 120

Yoachim, P., Roškar, R., & Debattista, V. P. 2010, ApJ, 716, L4

—. 2012, ApJ, 752, 97

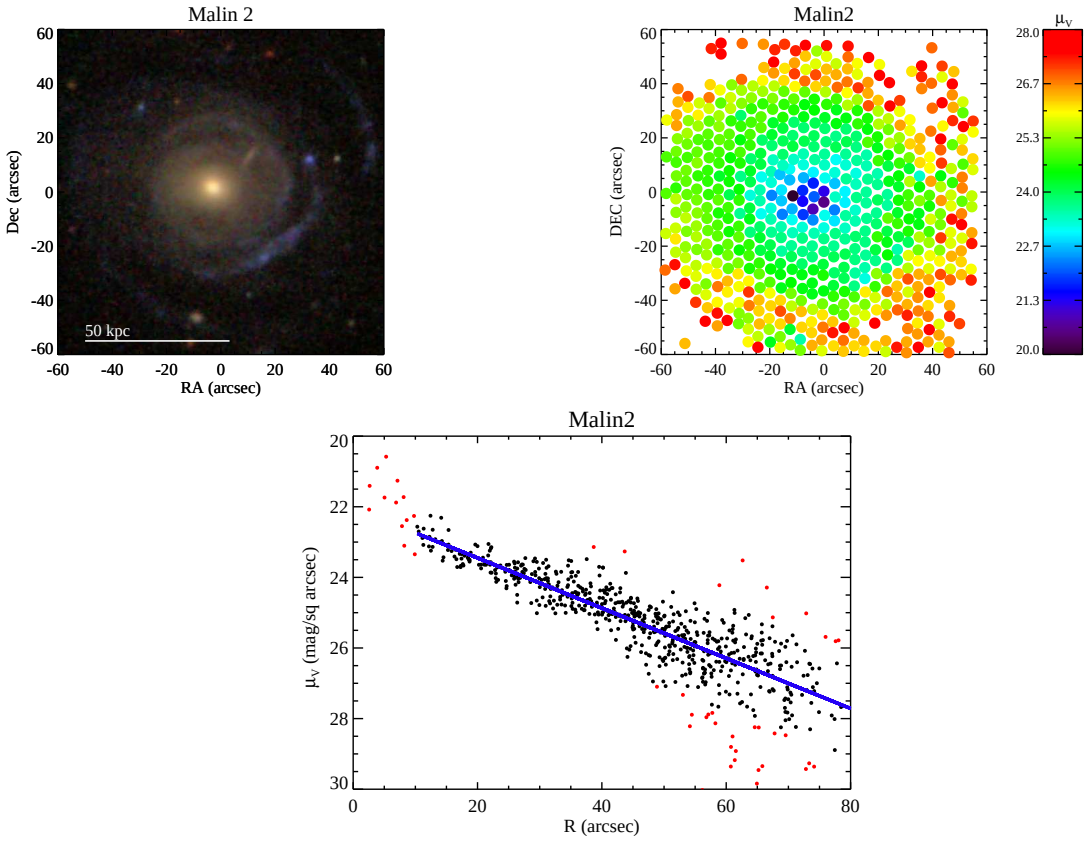

Fig. 4.— Upper Left: SDSS image of Malin 2. Upper Right: Image made with the VIRUS-P datacube. Lower: An exponential fit to the fiber magnitudes. Red points show fibers that were clipped while the solid line shows the best-fit.

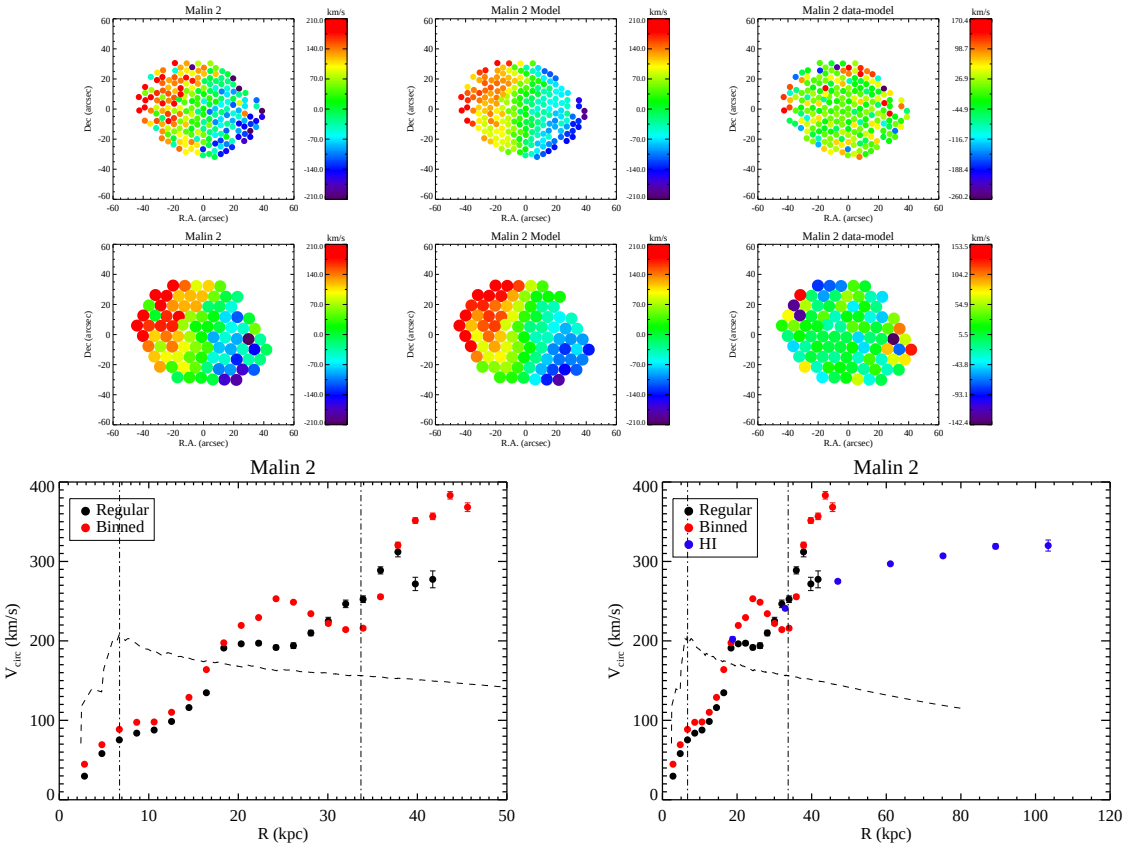

Fig. 5.— Fitting the line-of-sight velocity maps measured with Ppxf with the kinemetry package. The dashed curve shows the expected stellar mass contribution to the rotation curve. Vertical lines mark R_e and $5R_e$. H I data from Pickering et al. (1997).

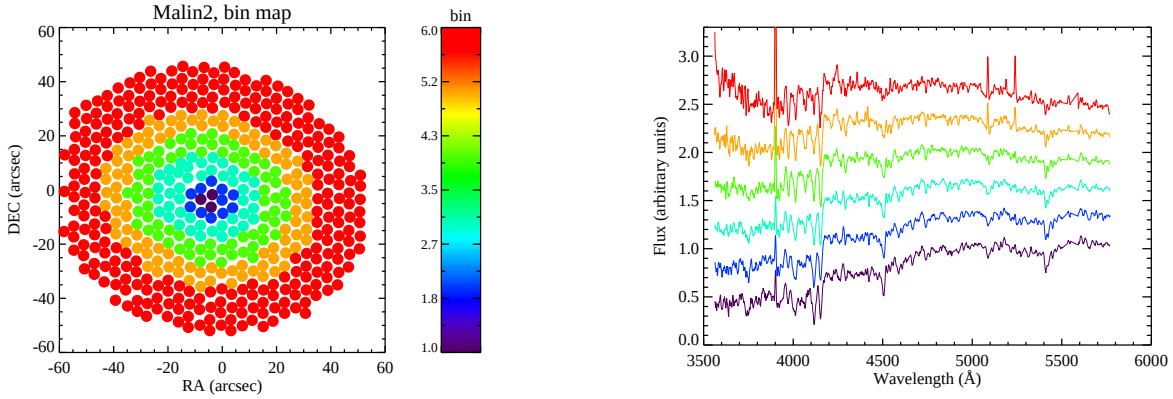

Fig. 6.— Left: Map of which fibers were binned together. Right: Resulting binned spectra, residuals from the bright skyline at 5577Å have been masked.

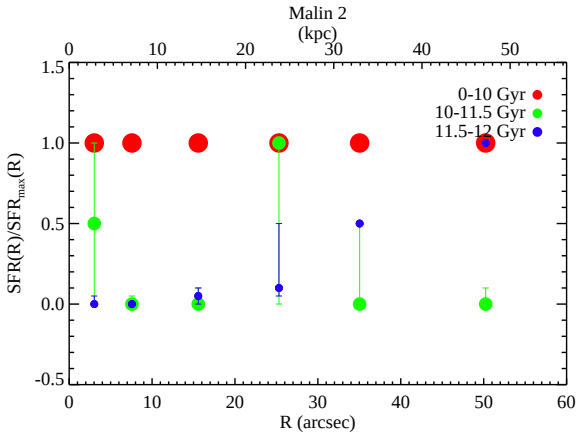

Fig. 7.— Best fitting star formation histories. For each bin, the SFH is normalized by the peak at each radius. Error bars are based on $\Delta\chi^2 = 100$ or the best fitting 4 models, whichever provides more points.

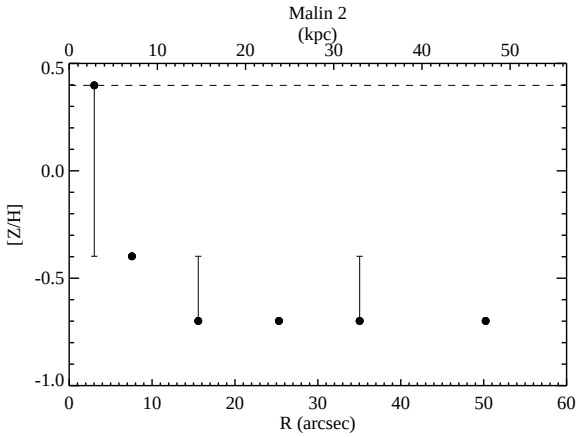

Fig. 8.— Best fitting stellar metallicities. Dashed line shows the maximum model metallicity used in the models (minimum is below the y range). Error bars are as in Figure 7.

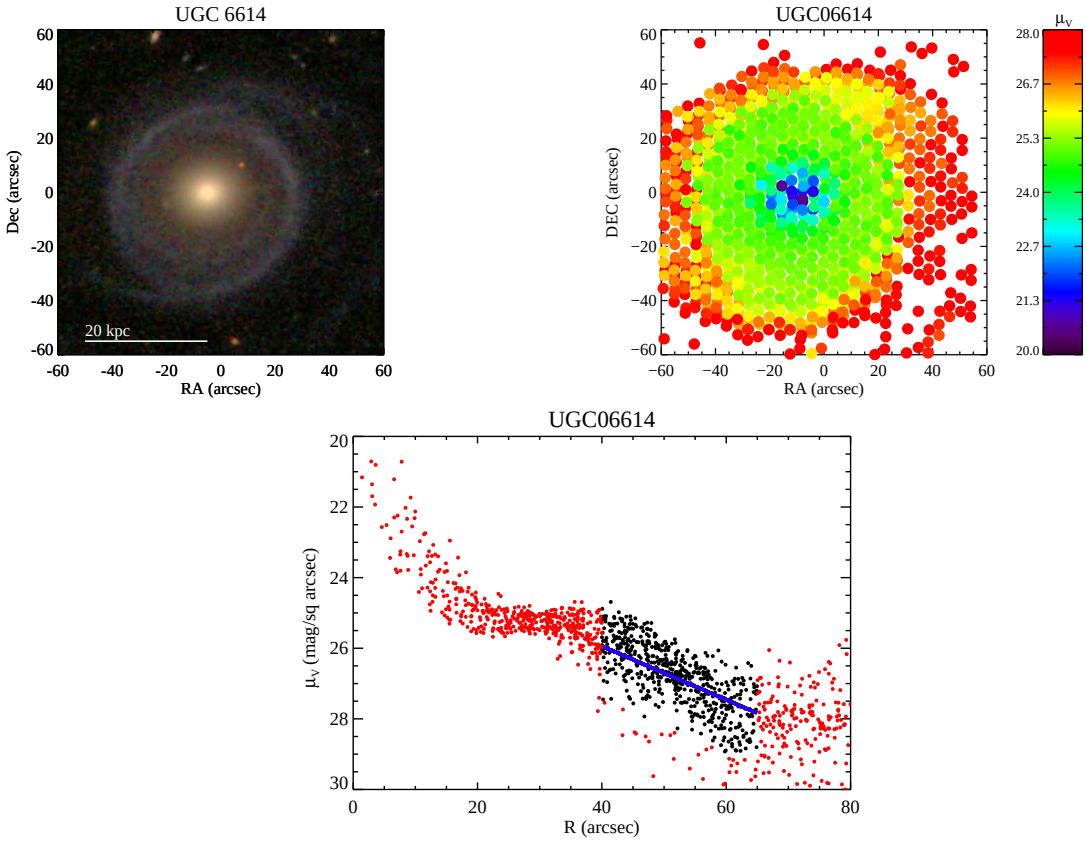

Fig. 9.— Upper Left: SDSS image of UGC 06614. Upper Right: Image made with the VIRUS-P datacube. Lower: An exponential fit to the fiber magnitudes. Red points show fibers that were clipped while the solid line shows the best-fit. We only included fibers beyond the outer ring structure.

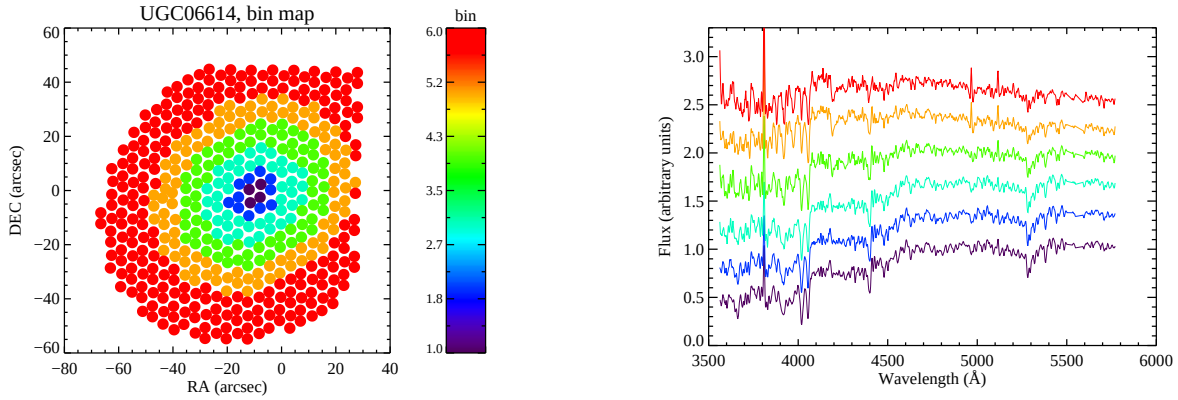

Fig. 10.— Left: Map showing which fibers were binned for UGC 6614. Right: The binned spectra, color-coded to match the map on the left.

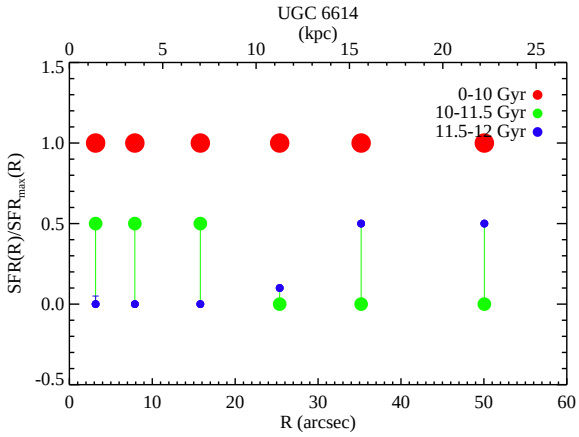

Fig. 11.— Best fitting star formation histories. For each bin, the SFH is normalized by the peak bin. Error bars are based on $\Delta\chi^2 = 100$ or the 4 best fitting models, whichever provides more points.

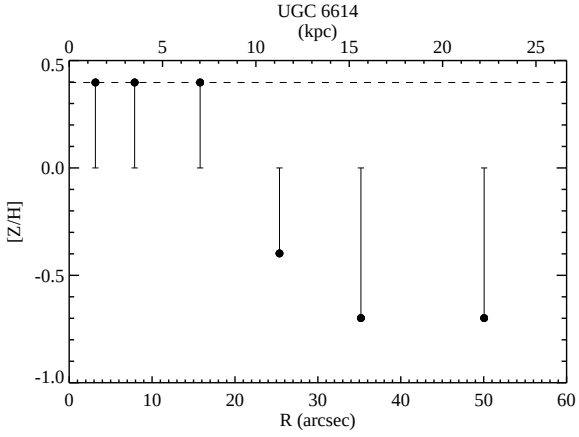

Fig. 12.— Best fitting stellar metallicities.

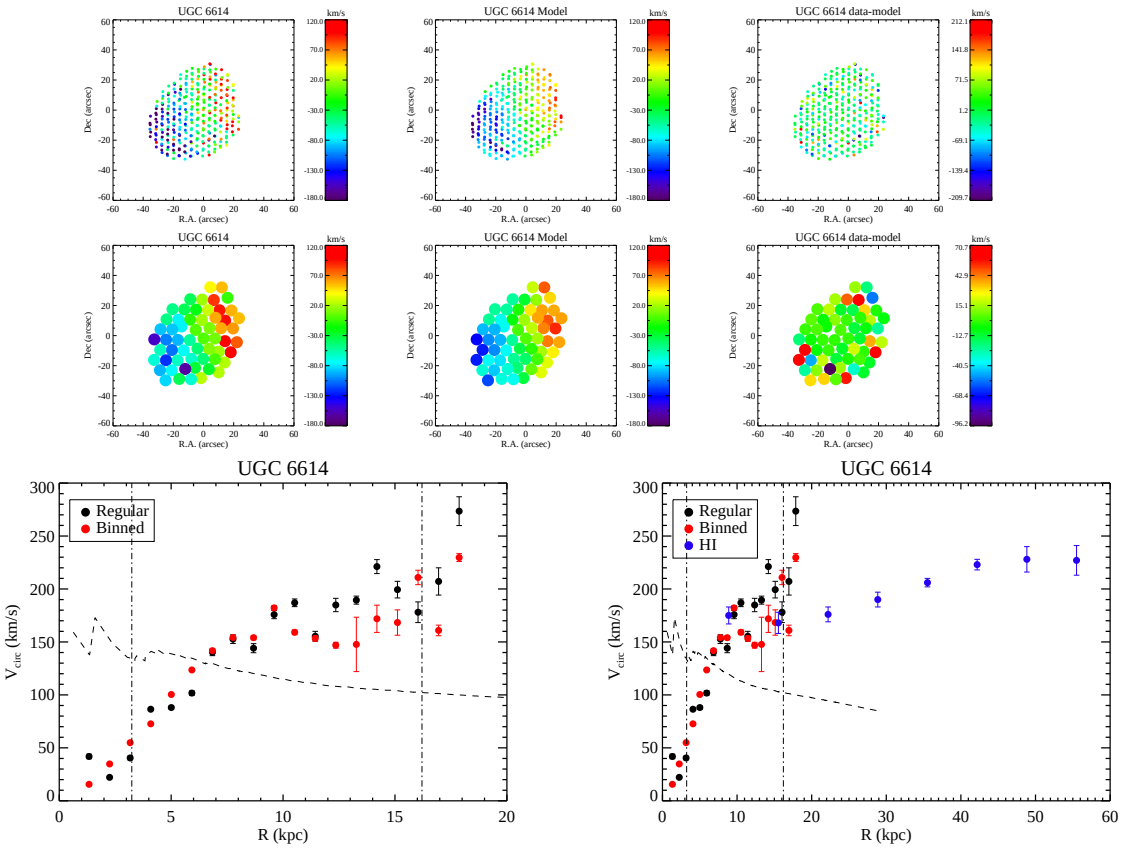

Fig. 13.— Fitting the velocity maps with kinemetry package. Vertical lines mark R_e and $5R_e$. The dashed lines shows a rotation curve based in the enclosed flux, normalized so that all the SDSS stellar mass is contained within $3R_e$. H I data from Pickering et al. (1997).

A. SDSS SQL quarries

To build our sample of comparison galaxies from SDSS, we used the CasJobs interface to query the SDSS DR10 database.

the galaxy CMD contours in Figure 1 were obtained via:

```
select
objid,ra,dec,
dered_u,dered_g,dered_r,dered_i,dered_z,
z,4.27E+3*z as d_hubble_mpc,
dered_u-dered_r as u_minus_r,
dered_r-5*log10(4.27E+8*z) as abs_mag_r

from specphotoall
where
class='GALAXY'
AND dered_r between 13.5 and 17.7
AND ((flags & 0x10000000) != 0)
AND ((flags & 0x8100000c00a0) = 0)
AND (((flags & 0x400000000000) = 0) or (psfmagerr_g <= 0.2))
AND (((flags & 0x100000000000) = 0) or (flags & 0x1000) = 0)
AND zerr < 0.05
AND z BETWEEN 0.01 and 0.085
AND dered_r - 5*log10(4.27E+08*z) BETWEEN -23.5 and -15.5
```

The Fundamental Plane contours in Figure 1 was computed from:

```
select
ph.objid, sp.z, sp.velDisp, sp.velDisperr, deVMag_g,deVMag_r, ph.deVRad_r,
ph.r,ph.dered_r, ph.extinction_r, ph.extinction_g, ph.deVAB_r,  gs.best_model_z,
gse.oh_p50, gse.lgm_tot_p50, gs.model_chisq_040, gs.model_chisq_080,
gs.model_chisq_170, gs.model_chisq_400, zoo.spiral, zoo.elliptical,
zoo.uncertain, zoo.p_el, zoo.p_cw,zoo.p_acw

from specobj as sp, photoobj as ph, galSpecIndx as gs,
galSpecExtra as gse, zoospec as zoo

where
```

```
sp.bestObjID = ph.objID and gs.specObjID = sp.specObjID
and gse.specObjID = sp.specObjID
and zoo.objid =  ph.objID

AND sp.class='GALAXY'
AND sp.velDisp != 0
AND sp.z BETWEEN 0.01 and 0.085
AND sp.zerr < 0.05
AND ph.dered_r between 13.5 and 17.7
AND ph.dered_u-ph.dered_r > 2.1
AND ph.lnLDeV_r-ph.lnLExp_r > 0.29559
AND ph.petroR90_i/ph.petroR50_i > 2.5
AND ((ph.flags & 0x10000000) != 0)
AND ((ph.flags & 0x8100000c00a0) = 0)
AND (((ph.flags & 0x400000000000) = 0) or (ph.psfmagerr_g <= 0.2))
AND (((ph.flags & 0x100000000000) = 0) or (ph.flags & 0x1000) = 0)
```

Finally, the mass-metallicity relation in Figure 1 was obtained via:

```
select
ph.objid,sp.velDisp, gse.lgm_tot_p50, gs.lick_hd_a_sub, gs.lick_hd_f_sub,
gs.lick_cn1_sub, gs.lick_cn2_sub, gs.lick_Ca4227_sub, gs.lick_G4300_sub,
gs.lick_hg_a_sub, gs.lick_hg_f_sub, gs.lick_fe4383_sub, gs.lick_ca4455_sub,
gs.lick_fe4531_sub, gs.lick_c4668_sub, gs.lick_hb_sub, gs.lick_fe5015_sub,
gs.lick_mg1_sub, gs.lick_mg2_sub, gs.lick_mgb_sub, gs.lick_Fe5270_sub,
gs.lick_Fe5335_sub, gs.lick_Fe5406_sub, gs.lick_Fe5709_sub, gs.lick_Fe5782_sub,
gs.lick_NaD_sub, gs.lick_TiO1_sub, gs.lick_TiO2_sub

from specobj as sp, photoobj as ph, galSpecIndx as gs, galSpecExtra as gse

where
sp.bestObjID = ph.objID and gs.specObjID = sp.specObjID
and gse.specObjID = sp.specObjID
AND sp.class='GALAXY'
AND sp.velDisp != 0
AND sp.z BETWEEN 0.01 and 0.085
AND sp.zerr < 0.05
AND ph.dered_r between 13.5 and 17.7
```

```
AND ph.dered_u-ph.dered_r > 2.1
AND ph.lnLDeV_r-ph.lnLExp_r > 0.29559
AND ph.petroR90_i/ph.petroR50_i > 2.5
AND ((ph.flags & 0x10000000) != 0)
AND ((ph.flags & 0x8100000c00a0) = 0)
AND (((ph.flags & 0x400000000000) = 0) or (ph.psfmagerr_g <= 0.2))
AND (((ph.flags & 0x100000000000) = 0) or (ph.flags & 0x1000) = 0)
```